

Ab Initio Transport Theory for Digital Ferromagnetic Heterostructures

Stefano Sanvito* and Nicola A. Hill

Materials Department, University of California, Santa Barbara, California 93106

(Received 24 August 2001; published 6 December 2001)

We present a theoretical density functional study of the electronic, magnetic, and transport properties of digital ferromagnetic heterostructures, obtained by δ doping GaAs with Mn. In the absence of intrinsic donors these systems have a half metallic density of states, with an exchange interaction much stronger than that of a random alloy with the same Mn concentration. Our *ab initio* ballistic transport calculations show that the carriers at the Fermi energy are strongly confined within a few monolayers around the MnAs plane. This strong confinement is responsible for the large exchange coupling and the two-dimensional half metallic behavior.

DOI: 10.1103/PhysRevLett.87.267202

PACS numbers: 75.50.Pp, 71.15.Mb, 73.23.Ad, 73.50.-h

Diluted magnetic semiconductors (DMS) based on III-V materials [1,2] are receiving great attention for the intriguing interplay between magnetic and electronic properties [3] and for the large potential for future electronic devices [4]. $\text{Ga}_{1-x}\text{Mn}_x\text{As}$, which is structurally compatible with most epitaxially grown III-V's, is the prototype of these materials. Here the Mn ions substitute randomly for the Ga ions, providing both localized $S = 5/2$ spins and free carriers (holes). The antiferromagnetic exchange coupling between the hole spin and the Mn spin is responsible for the long range ferromagnetic interaction, which can be described in a first approximation by the Zener model [5]. One important result of the model is that the Curie temperature is a linear function of the Mn concentration. Although the inclusion in the model of correlation effects [6] modifies this linear dependence, there is general agreement that an increase in the Mn concentration enhances the Curie temperature of the system.

Unfortunately, the solubility limit of Mn in GaAs is rather small, since MnAs naturally occurs in a hexagonal phase with [6]-coordinated Mn [7]. However large Mn concentration, up to 50% can be obtained in zinc blende MnAs submonolayers embedded into GaAs to form a MnAs/GaAs superlattice [8]. These structures, called digital ferromagnetic heterostructures (DFH) have remarkable properties. First, the Curie temperature decays for increasing GaAs interlayer thickness, and saturates for thicknesses larger than ~ 50 GaAs ML. The value of T_c at saturation depends on the Mn concentration [8]. A saturation is unexpected according to the Zener model for three-dimensional systems, since the total Mn concentration in the sample decreases with the increase of the GaAs thickness. This separation dependence suggests that DFH's behave like planar systems, although to date there is no direct proof that the free carriers responsible for the magnetic interaction are confined in the MnAs layers. Second, Hall measurements in the direction parallel to the MnAs planes show an anomalous Hall effect for undoped samples, which disappears upon Be doping [9,10]. Large Shubnikov de Haas oscillations are found in doped samples, although surprisingly the charge densities

extracted from the Hall coefficient and from the Shubnikov de Haas oscillations are different. This suggests that two different carrier types could be present in the system.

In this Letter we investigate theoretically the magnetic and transport properties of undoped DFH. In particular, we address the following questions: (i) What is the real dimensionality of the system? (ii) Are the carriers spin polarized? (iii) What is the carrier distribution in the system?

We perform density functional theory [11] calculations within the local spin density approximation using the Ceperley-Alder [12] form of the exchange-correlation potential. We use scalar relativistic Troullier-Martins pseudopotentials [13] with nonlinear core corrections and Kleinman-Bylander factorization. We choose the SIESTA implementation [14] because it uses a localized orbital basis set obtained from the numerical solution of the free atom pseudopotential, and a confining spherical potential of radius r_c . The cutoff radius r_c fixes the radial extension of the wave functions, which therefore are localized in space. This allows us to investigate systems with a large number of atoms. Further details of the method and its optimization have already been presented [15]. Each DFH superlattice is constructed by considering N GaAs cubic cells (8 atoms in the cell) aligned along the z direction (see Fig. 3c). One Ga plane is substituted with Mn and periodic boundary conditions are applied. This leads to an infinite $\text{MnAs}_1/\text{GaAs}_{2N-1}$ superlattice, where MnAs zinc blende monolayers are separated by a $5.65 \times N$ Å GaAs layer.

In Fig. 1 we present the band structure for the case $N = 8$ (with a 45.2 Å GaAs interlayer), for both the majority and minority spins. The points X_1 and X_2 are in the MnAs plane and denote directions along the edge and the diagonal of the cubic supercell, respectively. $\Gamma \rightarrow Z_1$ is the direction orthogonal to the MnAs plane. The band structure of Fig. 1 is that of a half metal, with a gap of approximately 0.65 eV in the minority spin band. The majority spin band presents a strongly anisotropic dispersion. It is metallic and quite dispersive in the MnAs plane (directions $X_1 \rightarrow \Gamma \rightarrow X_2$), while in the direction

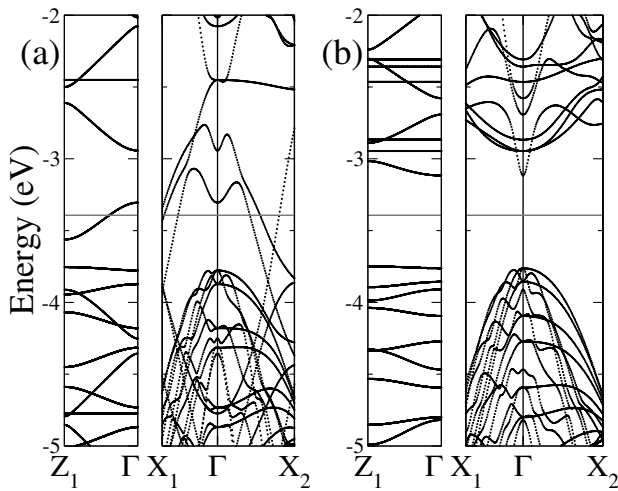


FIG. 1. Band structure for a $\text{MnAs}_1/\text{GaAs}_{15}$ superlattice: (a) majority and (b) minority spins. X_1 and X_2 are in the MnAs plane and denote directions along, respectively, the edge and the diagonal of the cubic supercell. $\Gamma \rightarrow Z_1$ is the direction orthogonal to the MnAs plane. The horizontal line indicates the Fermi energy.

orthogonal to the MnAs plane there is the formation of a narrow impurity band. Since the Fermi energy E_F cuts through the impurity band, MnAs/GaAs looks like a two-dimensional half metal with small hopping between the MnAs planes. The width of the impurity band decreases with increasing separation between the MnAs planes (665 meV, 412 meV, and 256 meV, respectively, for $N = 4$, $N = 6$, and $N = 8$), which is consistent with the decrease of the overlap between the wave functions centered on the MnAs planes [16].

We calculate the strength of the magnetic coupling by calculating the difference Δ_{FA} between the total energy of supercells with either antiferromagnetic or ferromagnetic alignment of the Mn ions [17]. We find that the ferromagnetic interaction is much stronger than that in a random alloy with the same Mn concentration. For instance in the $\text{MnAs}_1/\text{GaAs}_{15}$ DFH with a Mn concentration of $x = 0.06$, Δ_{FA} is 515 meV, whereas in the corresponding random alloy it is only 160 meV. Moreover, Δ_{FA} seems to be rather independent of the GaAs thickness for the range of thicknesses investigated here (531, 533, and 515 meV, respectively, for $N = 4$, $N = 6$, and $N = 8$), suggesting that the carriers responsible for the ferromagnetism are indeed strongly confined in the MnAs planes.

We also investigate the effect of introducing As antisites (As_{Ga}) by considering a $\text{MnAs}_1/\text{GaAs}_{11}$ superlattice with $1/2$ ML of As_{Ga} close to the MnAs plane. This corresponds to one As_{Ga} for two Mn, hence according to the nominal valence, to compensation. In contrast to what is expected from the Zener model, the coupling between the Mn ions is still ferromagnetic with $\Delta_{\text{FA}} = 70$ meV. This result is similar to that found for the tetrahedral $\text{Ga}_1\text{Mn}_2\text{As}_2$ complex in GaAs [17], although in that case $\Delta_{\text{FA}} = 20$ meV. We interpret the ferromagnetism

at compensation in the presence of As_{Ga} as being due to localized carriers Zener-coupled to the Mn ions [17]. The MnAs/GaAs superlattices have stronger ferromagnetic coupling than that of the $\text{Ga}_1\text{Mn}_2\text{As}_2$ complex since the carrier localization close to the MnAs plane is very strong. These results suggest that also in DFH the Curie temperature is determined by a delicate interplay between Mn ions and intrinsic defects.

We now move to the transport properties. Here we generalize the technique of Ref. [18] to the case of nonorthogonal tight binding model with singular coupling matrices. The conductance is calculated in the ballistic limit with both the current in the Mn plane (CIP) and perpendicular to the Mn plane (CPP). We first compute the tight-binding Hamiltonian and overlap matrix giving the correct charge density. The basis set is the localized atomic orbital basis set used for the self-consistent procedure. The matrix elements are computed by evaluating two and three center integrals with a numerical integration over a real space grid [14]. Note that in this way the Hamiltonian and the overlap matrix are computed exactly within the density functional calculation over the localized basis set. The resulting tight-binding Hamiltonian comprises in principle an arbitrary large number of nearest neighbor interactions. In practice, the number of atomic orbitals interacting with a given one is fixed by the size of the basis set cutoff radius. We then rewrite both the Hamiltonian and the overlap matrix in a tridiagonal form along the direction of the transport, using periodic boundary conditions for the other directions. This transforms the problem into a set of quasi-one-dimensional k -dependent problems. The finite interaction range between the atomic orbitals allows us to define the unit cell for the tridiagonal form so that each unit cell is coupled only to nearest neighboring cells. The scattering matrix is then calculated by a well-established Green's function technique [18], and the spin conductance Γ_σ by using the Landauer-Büttiker formula [19] and integrating over the two-dimensional Brillouin zone in the plane orthogonal to the direction of transport,

$$\Gamma_\sigma = \frac{e^2}{h} \sum_k^{\text{BZ}} \text{Tr} t_\sigma(k) t_\sigma(k)^\dagger. \quad (1)$$

Here $t_\sigma(k)$ is the k -dependent transmission matrix for the spin σ . We assume a two spin fluid model where there is no mixing between majority and minority spins. It is important to point out that in the CPP case our supercell geometry leads to narrow bands. It is then crucial to perform large k_{\parallel} -point sampling. Here we consider up to 800 k_{\parallel} points in the two-dimensional irreducible Brillouin zone.

In Fig. 2 we present the conductance per unit area as a function of the position of the Fermi energy for a $\text{MnAs}_1/\text{GaAs}_{15}$ superlattice for both the CIP and CPP directions and both spins. We also project the conductance onto the atomic orbital basis set in order to determine the orbital character of the electrons carrying the current [18].

If we now analyze closely the conductance of the majority spin band we notice that it is strongly anisotropic,

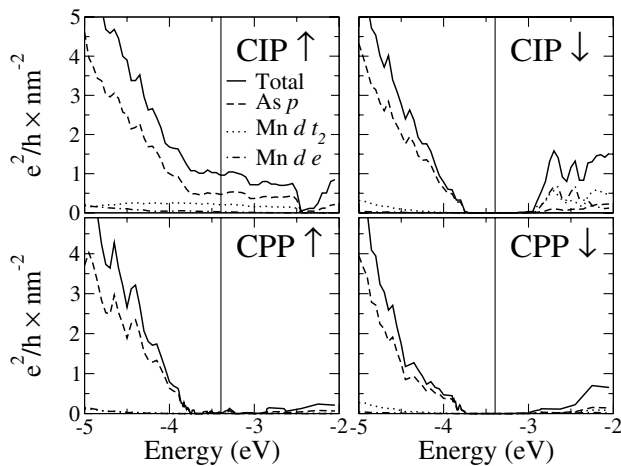


FIG. 2. Total and partial conductance per unit area for a $\text{MnAs}_1/\text{GaAs}_{15}$ superlattice as a function of the position of the Fermi energy for majority (\uparrow) and minority (\downarrow) spin bands. The vertical line denotes the position of the Fermi energy for undoped samples.

as expected from the band structure of Fig. 1. In the CIP direction the conductance as a function of the position of the Fermi energy is rather flat with an orbital contribution mainly from the As p orbital. There is also a significant contribution (roughly 20% of the total conductance) coming from the Mn dt_2 orbitals, suggesting that the carriers in undoped samples are confined close to the MnAs planes. It is also important to point out that in k space the contributions to the conductance are rather uniformly distributed over the two-dimensional Brillouin zone in the plane orthogonal to the transport direction. These are strong indications that MnAs/GaAs is a good isotropic metal in the MnAs planes.

For the CPP direction the situation is rather different. The conductance as a function of the position of E_F shows clear one-dimensional features and for undoped samples it is solely given by charge in the impurity band. The orbital content of the impurity band is mainly As p with small contributions from Mn $d t_2$. The conductance at E_F comes from a few k points around the Γ point. In the case of carriers with parabolic dispersion this happens for scattering at a potential barrier, when the carrier energy is very close to the top of the barrier. In fact, carriers with largest kinetic energy in the direction orthogonal to the barrier (small k in the parallel direction) have largest transmission amplitude. This situation is similar to that of tunneling junctions, and so we describe the transport as tunneling-like.

We now turn our attention to the minority spin band, where it is clear that the conductance vanishes within a 1 eV wide region around E_F . Therefore there is 100% spin polarization of the conductance for undoped samples (E_F is in the gap for the minority spin). Moreover, we have calculated the position of the GaAs valence band edge and found that this lies in the gap of the minority band. This means that in an DFH/GaAs heterostructure we have

100% spin polarization at an energy corresponding to the GaAs valence band edge. For this reason DFH appear as good candidates for spin injection into p -doped GaAs.

In summary, from ballistic transport calculations, MnAs/GaAs appears to be a two-dimensional half metal in the MnAs plane, with tunneling-like conductance between the MnAs planes. In order to better understand the spatial arrangement of the current in Fig. 3 we present the charge density distribution in real space $\rho(\mathbf{r})$, calculated only for those states contributing to the conductance and within a 0.6 eV range around E_F ($E_F - 0.3 \text{ eV} < E < E_F + 0.3 \text{ eV}$). We also notice that the individual contributions from occupied ($E_F - 0.3 \text{ eV} < E < E_F$) and unoccupied ($E_F < E < E_F + 0.3 \text{ eV}$) states are very similar.

The figure confirms that the current in the CIP case is distributed mainly in a narrow region around the MnAs planes, with small spillage outside. Planar averaging [20] of the charge density of Fig. 3 shows that the charge density reaches ~ 0.1 of its MnAs plane value within only three GaAs monolayers from the MnAs plane. In contrast, the CPP current is mainly located at the Mn plane with small contributions from the GaAs layers. This means that carriers are strongly confined in the MnAs plane and the perpendicular transport is via hopping between the planes.

Finally, in Fig. 4 we present the macroscopic average [20] of the Hartree potential. The macroscopic average is obtained by first taking a planar average and then by averaging the result over the GaAs lattice spacing. This does not correspond exactly to the total potential which

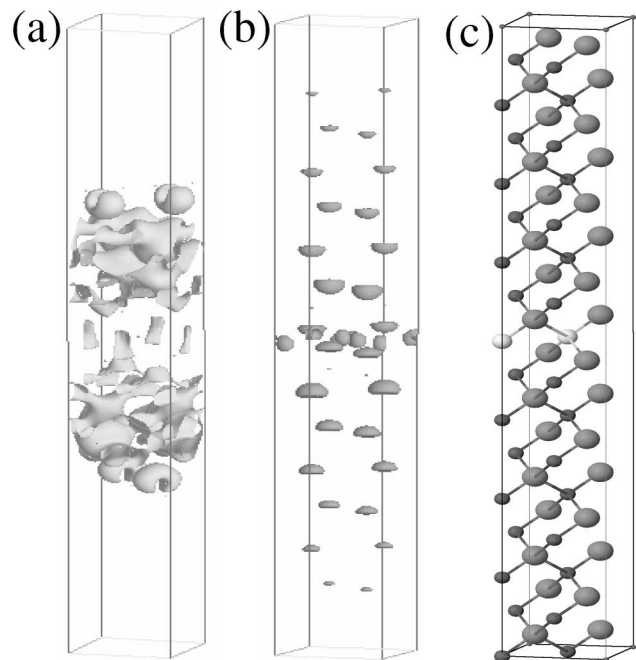


FIG. 3. Charge density distribution in real space for $\text{MnAs}_1/\text{GaAs}_{15}$ calculated only for those states contributing to the conductance and energy within 0.3 eV from E_F : CIP (a) and CPP (b) configurations. In (c) the scheme of the supercell.

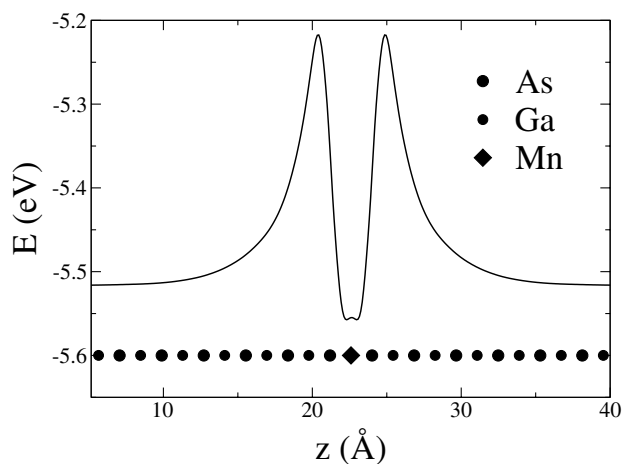


FIG. 4. Macroscopic average of the Hartree potential for $\text{MnAs}_1/\text{GaAs}_{15}$.

the quasiparticles feel in the structure, but it gives a good indication of the latter [20]. The potential profile shows a deep well in the MnAs plane separated from a flat region by two barriers located 1 ML from the well. The presence of the barrier suggests that n -type doping in the GaAs region will only weakly affect the MnAs planes, since the extra electrons need to tunnel through a large barrier to access the MnAs planes.

In conclusion, we have studied with *ab initio* methods the magnetic and transport properties of GaAs/MnAs DFH. We have shown that they are two-dimensional half metallic systems with large metallic conductance in the MnAs plane, and small tunneling-like conductance perpendicular to the MnAs plane. We have shown that the electronic charge at the Fermi energy is mainly distributed within a few ML around the MnAs plane and that the Hartree potential shows a double barrier profile. This potential profile can sustain the presence of a two carrier population for DFH's that are Be doped in the GaAs region.

We thank E. Gwinn and E. Johnston-Halperin for stimulating discussions. This work made use of MRL

Central Facilities supported by the National Science Foundation (No. DMR96-32716). This work is supported by ONR (N00014-00-10557), by NSF-DMR (9973076), and by ACS PRF (33851-G5).

*Electronic address: ssanvito@mrl.ucsb.edu

- [1] H. Ohno, J. Magn. Mater. **200**, 110 (1999), and references therein.
- [2] H. Ohno, Science **281**, 951 (1998).
- [3] H. Ohno *et al.*, Nature (London) **408**, 944 (2000).
- [4] G. Prinz, Science **282**, 1660 (1998).
- [5] T. Dietl *et al.*, Science **287**, 1019 (2000).
- [6] A. Chattopadhyay, S. Das Sarma, and A.J. Millis, Phys. Rev. Lett. **87**, 227202 (2001).
- [7] S. Sanvito and N.A. Hill, Phys. Rev. B **62**, 15 553 (2000).
- [8] R.K. Kawakami *et al.*, Appl. Phys. Lett. **77**, 2379 (2000).
- [9] G. Zanelatto *et al.*, Bull. Am. Phys. Soc. **46**, 509 (2001).
- [10] T. Kreutz *et al.*, Bull. Am. Phys. Soc. **46**, 510 (2001).
- [11] H. Hohenberg and W. Kohn, Phys. Rev. **136**, B864 (1964); W. Kohn and L. Sham, Phys. Rev. **140**, A1133 (1965).
- [12] D.M. Ceperley and B.J. Alder, Phys. Rev. Lett. **45**, 566 (1980).
- [13] N. Troullier and J.L. Martins, Phys. Rev. B **43**, 1993 (1991).
- [14] D. Sánchez-Portal, P. Ordejón, E. Artacho, and J.M. Soler, Int. J. Quantum Chem. **65**, 453 (1997), and references therein.
- [15] S. Sanvito, P. Ordejón, and N.A. Hill, Phys. Rev. B **63**, 165206 (2001).
- [16] J. Fernández-Rossier and L.J. Sham, cond-mat/0106548.
- [17] S. Sanvito and N.A. Hill, Appl. Phys. Lett. **78**, 3493 (2001).
- [18] S. Sanvito, C.J. Lambert, J.H. Jefferson, and A.M. Bratkovsky, Phys. Rev. B **59**, 11 936 (1999).
- [19] M. Büttiker, Y. Imry, R. Landauer, and S. Pinhas, Phys. Rev. B **31**, 6207 (1985).
- [20] S. Baroni, R. Resta, A. Baldereschi, and M. Peressi, in *Spectroscopy of Semiconductor Nanostructures*, edited by G. Fasol, A. Fasolino, and P. Lugli (Plenum, New York, 1989), p. 251.